On the Formation of Pipes and Centerline Segregates in Continuously Cast Billets

C.-M. RAIHLE and H. FREDRIKSSON

Centerline macrosegregation in continuously cast steel billets, blooms, and slabs is a significant problem. Thermal contraction of the solidified shell at the final end of the liquid pool causes a separation in the central portion of the strand and formation of a pore. When this pore fills with liquid, centerline macrosegregation results. Segregation formation is influenced by the cooling and casting conditions. The effects of those parameters are discussed in this article. Thermal contraction also causes formation of a large pipe in the very last portion of the strand. The casting parameters that control the centerline macrosegregation also control the size of the pipe.

I. INTRODUCTION

CENTERLINE porosity and macrosegregation are two of the most severe problems encountered in continuous casting of steel billets and slabs. Centerline macrosegregation is an uneven distribution of alloying elements across the centerline axis, usually with a positive segregation (concentration peak above the average concentration) of alloying elements in the center of the strand and a negative segregation (concentration less than average) on both sides. The formation of these types of defects has been discussed extensively in the literature.[1-4] Earlier it was believed that centerline macrosegregation as well as centerline porosity are caused by the fact that steel decreases in volume when solidifying due to the phase transformation from liquid to solid, *i.e.*, solidification shrinkage. However, some years ago it was proposed that centerline macrosegregation is caused by thermal contraction of the solidified shell during solidification of the central portion of the strand.[4] This thermal contraction is caused by the temperature decrease in the solidified shell. It is difficult to verify experimentally which of these two factors is dominant during a casting operation.

A distinction between the two factors can be made by analyzing the formation of the pipe in the last portion of the strand to be cast. Pipes are usually associated with ingot casting and are normally disregarded in continuous casting of steel. However, at the end of a casting sequence, a pipe is formed in the very last portion of the strand solidified.

The section of the strand that contains the pipe cannot be used and thus must be remelted, resulting in a lower yield. A better understanding of the factors that influence pipe formation should lead to methods of decreasing the pipe depth and increasing the yield in continuous casting, which is beneficial from an economic viewpoint.

Pipes formed during a casting operation are caused by thermal contraction as well as by solidification shrinkage. During ingot casting, contraction and volume change cause a decrease in liquid volume. As a consequence, the liquid surface level will decrease at the top of the ingot. During a continuous casting process, liquid is continuously supplied to the mold and compensates for the volume decrease. This situation changes at the end of a continuous casting operation, when feeding of liquid metal from tundish to mold ceases. Then the conditions are similar to those for ingot casting, and a pipe will form.

The pipe is very well developed in billets, but not so pronounced in slabs. This can be attributed to differences in casting conditions and in construction of the equipment used to produce the two types of products. The discussion in this article will be limited to the casting of billets.

The volume of the liquid pool as well as the thermal contraction can be affected by variations in the casting parameters. The aim of this article is to present a model to simulate pipe formation. The model will use reasonable approximations to solve a very complex problem. The calculated values are compared with experimental results. The influence of different casting parameters on the pipe is investigated, and an ideal finishing procedure for continuous casting is discussed.

During the casting operation, liquid flows into the contracting and shrinking parts of the strand—a process that causes macrosegregation. The article will conclude with a discussion of how centerline macrosegregation and centerline porosity are related to thermal contraction and pipe formation.

Alloy composition also influences pipe formation. Solidification shrinkage, thermal expansion coefficient, thermal conductivity, latent heat, heat capacity, and thermal contact resistance at the mold/strand surface vary with different alloy compositions. We have not studied the effects of these parameters.

II. EXPERIMENTAL RESULTS

A number of experiments were carried out using Koverhar Dalsbruks OY's continuous casting machine. The experiments are more fully described in References 4 and 5. Only some of the experimental results will be presented in this article. Figure 1 shows a schematic illustration of the machine. In the experiments, the casting

C.-M. RAIHLE, Postgraduate Student, and H. FREDRIKSSON, Professor, are with the Department of Casting of Metals, Royal Institute of Technology, Stockholm S-100 44, Sweden.

Manuscript submitted June 24, 1991.

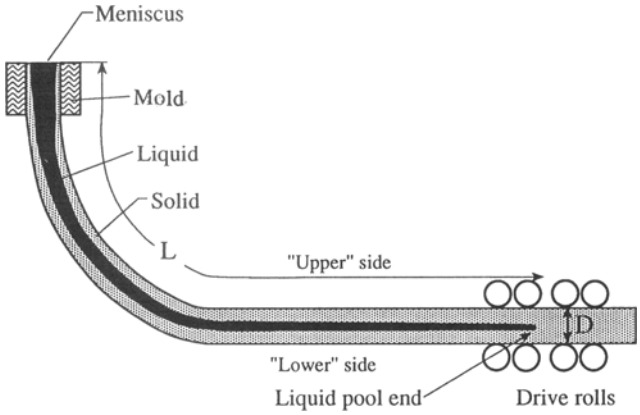

Fig. 1—Schematic illustration of the continuous casting equipment used. The secondary cooling is divided into four or five zones in the two machines. *L* is the liquid pool length. The drive rolls are also shown.

speed and cooling conditions were varied in order to obtain a variety of data for testing the numerical model. The different casting conditions and the material data for the experiments discussed here are shown in Tables I through VI. For the analysis of pipe formation, a 0.1 pct carbon steel was used; for the discussion of macrosegregation, a 0.8 pct carbon steel was used. The basic

Table I. Experimental Casting Parameters

Experiment Number	Billet Size (mm^2)	Casting Speed (m/min)	Casting Speed during Pipe Formation (m/min)	Casting Temperature (K)
1	130 × 130	1.9	1.2	1842
2	115 × 115	2.7 to 2.25*	2.55	1845

*In experiment 2, the normal casting speed was decreased from 2.7 to 2.25 m/min over a period of 8 min.

Table II. Length of Cooling Zones

Zone	Length, Experiment 1 (m)	Total Length, Experiment 1 (m)	Length, Experiment 2 (m)	Total Length, Experiment 2 (m)
Mold	0.7	0.7	0.7	0.7
I	0.15	0.855	0.43	1.13
II	1.15	1.9	0.685	1.815
III	2.55	4.45	1.385	3.2
IV	1.45	5.9	2.6	5.8
V	0.9	6.8	—	—

Table III. Material Data

Liquidus temperature	1783 K
Solidus temperature	1728 K
Latent heat	270 kJ/kg
Heat capacity	620 J/kg
Density	7500 kg/m^3
Heat conductivity	28 W/mK
Thermal expansion coefficient	1.4×10^{-5}

mechanisms that cause pipe formation and centerline macrosegregation are independent of the cast material. It is thus possible to draw parallels between the two experimental series despite the different carbon contents.

Pipe formation at two different casting speeds—1.9 and 2.7 m/min—will be discussed (Table I). After casting, the end portions of the strands were cut into equal longitudinal halves, and the shape of the pipe was documented and measured by sulfur prints (Figure 2). The measurements were made on the upper side of the strand to avoid the sedimented equiaxed crystals.

For the sample cast at a speed of 2.7 m/min, the segregation around and along the centerline was measured in the strand. The metallographic evaluation was performed using samples macroetched with hot hydrochloric acid. Specimens for chemical analyses were extracted by milling at various distances from the strand surface; the dimensions of the milled samples were 2 × 2 × 40 mm, and the distance between each sample was 2 mm. Results of the segregation analysis are shown in Figure 3. The macrostructure of the billet consists of columnar crystals at the surface and equiaxed crystals around the centerline; a linear analysis indicates about 20 pct equiaxed crystals. The equiaxed crystal zone is somewhat displaced toward the lower side of the strand; this is natural since the equiaxed crystals sediment due to gravity when the strand turns horizontally in a bent machine.

The segregation analysis shows a very heavy centerline macrosegregation just below the end of the pipe represented by the curve in Figure 3(a). The macrosegregation along the centerline then decreases; this may be part of a periodic variation reported earlier by Mori *et al.*[1] Other concentration peaks are also visible in Figure 3, perhaps caused by V-segregates or other inhomogeneities in the structure. Sulfur prints were made on the samples to locate the centerline, but the macrostructure was not studied. We did not expect such inhomogeneities and thus cannot provide clear explanation of these concentration peaks at the side of the centerline macrosegregation. The variations of the centerline macrosegregation can be related to the formation of V-segregates. This was illustrated by a series of nailing experiments,[4] in which a hollow nail filled with FeS was shot into the strand, allowing the liquid flow to be characterized by the sulfur distribution on an etched sample.

This variation in centerline macrosegregation may also be the result of thermal shrinkage;[4,5] *i.e.*, during solidification of the last portion of the strand, liquid is transported downward in the strand. The relatively large effect at the end of the casting process directly under the pipe can be attributed to the fact that the temperature drop at the center is much more rapid when the last liquid solidifies than during steady-state casting conditions.

Figure 4 shows an example where a nail has been shot into the strand just before the liquidus fronts meet in the central portion of the strand. The corresponding segregation analysis is shown in Figure 5. In this case, the nail has blocked the central region before the liquid farther down has solidified. Figure 4 shows that a bridge has been formed, below which a large pore is visible. Liquid has been transported downward to replace the

Table IV. Steel Compositions (Weight Percent)

Experiment Number	C	Si	Mn	P	S	Cr	Mo	V
1	0.09	0.07	0.88	0.032	0.012	0.0325	0.002	0.045
2	0.11	0.24	0.58	0.021	0.033	0.053	0.006	0.023

Table V. Casting Speeds and Heat-Transfer Coefficients for Experiment 1

Casting Speed (m/min)	Heat-Transfer Coefficient (W/m^2 K) in Zone:						
	Mold	I	II	III	IV	V	∞
1.2	1300	1120	660	400	330	225	120
1.9	1300	1411	830	512	426	289	120

Table VI. Heat-Transfer Coefficients for Experiment 2

Zone	Heat-Transfer Coefficient (W/m^2 K)
Mold	1300
I	1126
II	785
III	575
IV	297
V	120

space left by solidification and thermal shrinkage. Liquid has flowed from the area above the bridge through the network of solid/liquid, forming a U-shaped segregate. The region at the bridge or around the bridge consists of purer material. At a point 3 cm above the bridge, the central portion has a high positive segregation (Figure 5). The segregation 10 cm below the nail at the end of the pore is slightly positive in the central portion (Figure 5). Far below the end of the pore, the segregation pattern resembles the one shown 3 cm above the nail, which is the normal segregation pattern in billets.

The downflow of liquid during solidification of the center was demonstrated by the nailing experiments mentioned earlier. The nails contained iron sulfide, and the flow was visualized by a sulfur print (Figure 6). Two types of flow were observed. One was mainly downward and slightly inward to the center; the other was directed sharply inward following the V-segregation lines. It is proposed that these two convection modes are formed during two different periods of the solidification process, as will be discussed later.

III. MODEL DESCRIPTION FOR PIPE FORMATION

In ingots, solidification shrinkage is the dominant factor in pipe formation. This has been investigated by, among others, Brolund *et al.*[6] A simple material balance shows that the pipe in a strand is normally much deeper than can be accounted for by solidification shrinkage. In order to explain pipe formation in continuous casting, the effects of thermal shrinkage must also be included, as has been discussed by the present authors.[5] The model for pipe formation in a strand caster

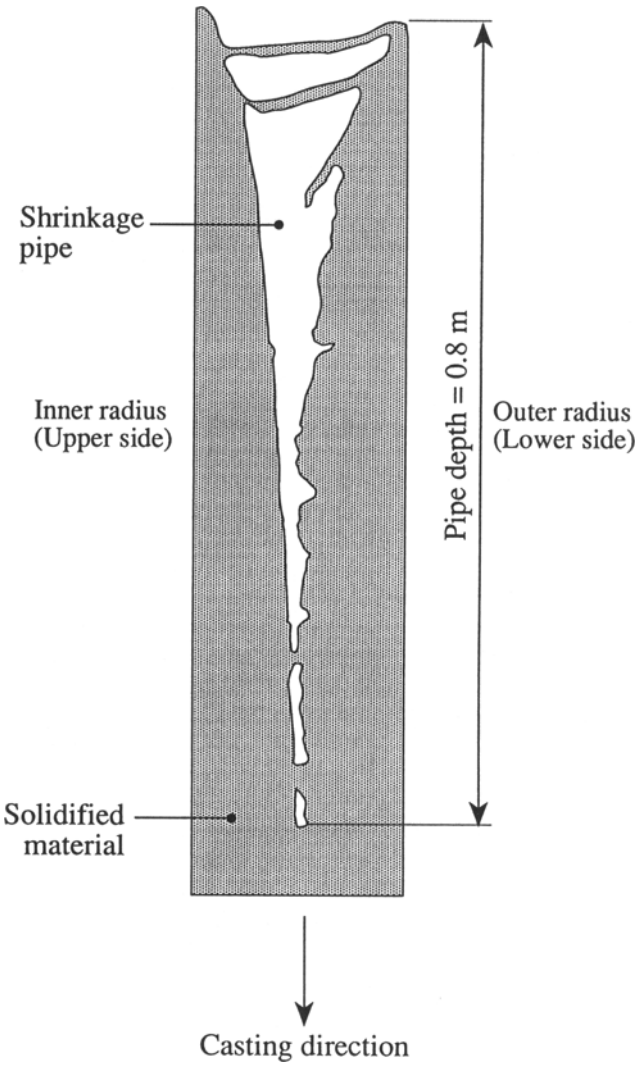

Fig. 2—Shrinkage pipe formed at the end of the casting operation (sketched from a sulfur print). The pipe was measured on the inner radius (upper side) of the strand.

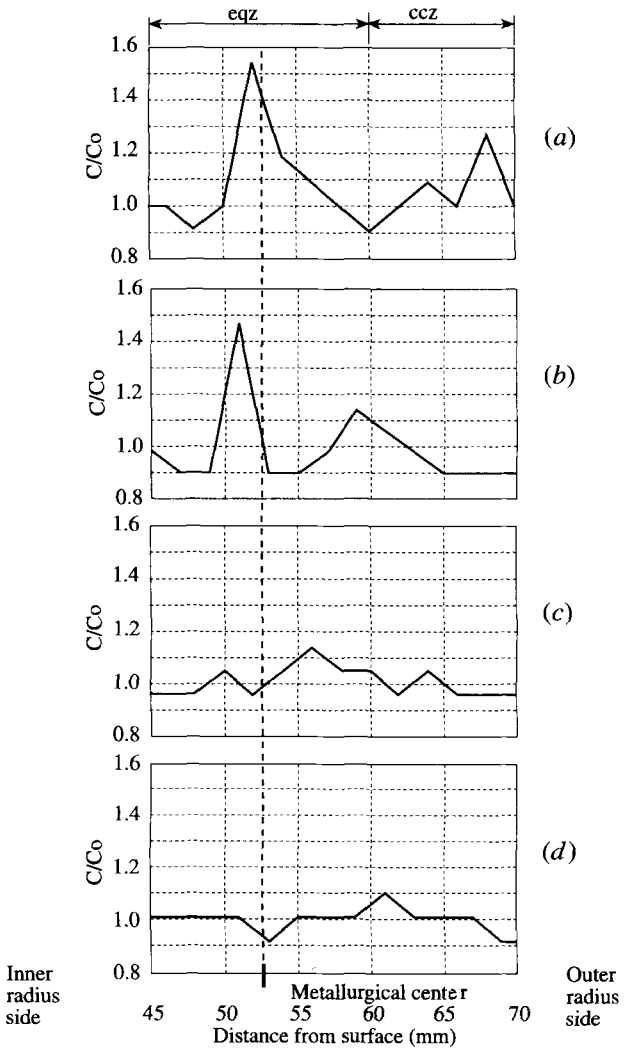

Fig. 3—Carbon segregation at various distances below the pipe: (*a*) 2.5 cm; (*b*) 6.5 cm; (*c*) 15 cm; and (*d*) 23.5 cm. The metallurgical centerline is located 52.5 mm from the upper side of the strand, *i.e.*, somewhat displaced toward the upper side. eqz, equiaxed crystal zone; ccz, columnar crystal zone.

can also be based on a material balance, described with the help of Figure 7—a schematic view of the strand where the liquid surface and the position of the solidification front are shown at two different times, t and $t + \Delta t$. The volume ΔV_s has solidified during the time Δt; this causes a certain volume to disappear due to solidification shrinkage. During the time Δt, the solidified shell contracts thermally, with a resulting change in volume, ΔV_c.

As a consequence of these two volume changes, the position of the liquid surface will change. Normally the surface will move downward, in a positive z-direction, a distance of Δh. The material balance can be expressed by a differential equation as

$$\frac{dh}{dt} A_s = \frac{dV_s}{dt} \beta + \frac{dV_c}{dt} \qquad [1]$$

where dh is the difference in the position of the metal liquid surface (m), A_s is the area of the metal liquid surface (m^2), dV_s is the difference in the solidified volume

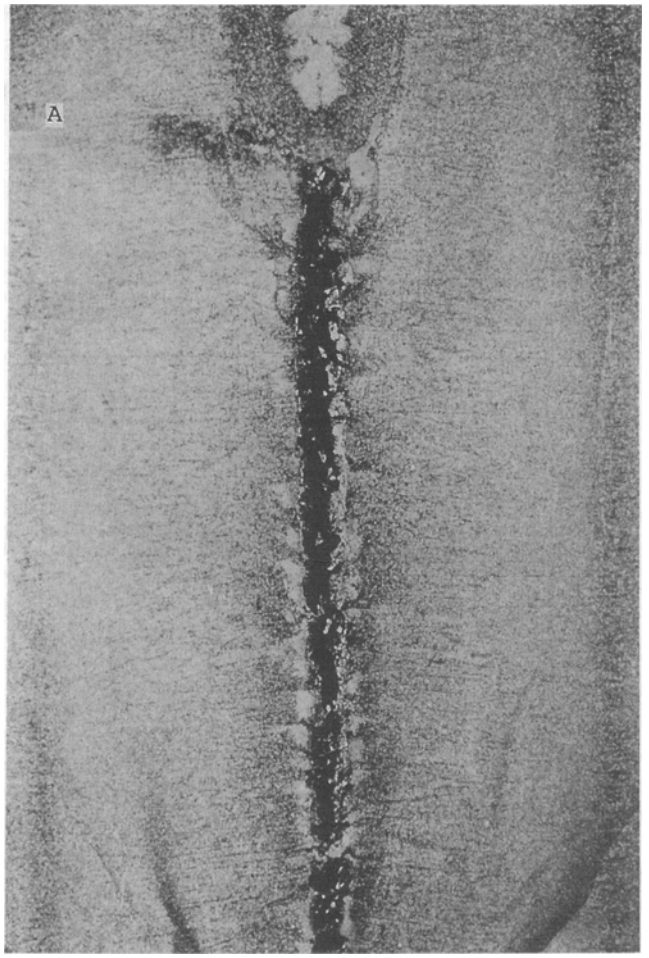

Fig. 4—Pore formation in the central portion of a strand illustrated by a nailing experiment.[4] The position of the nail is indicated by A. Magnification 1 times.

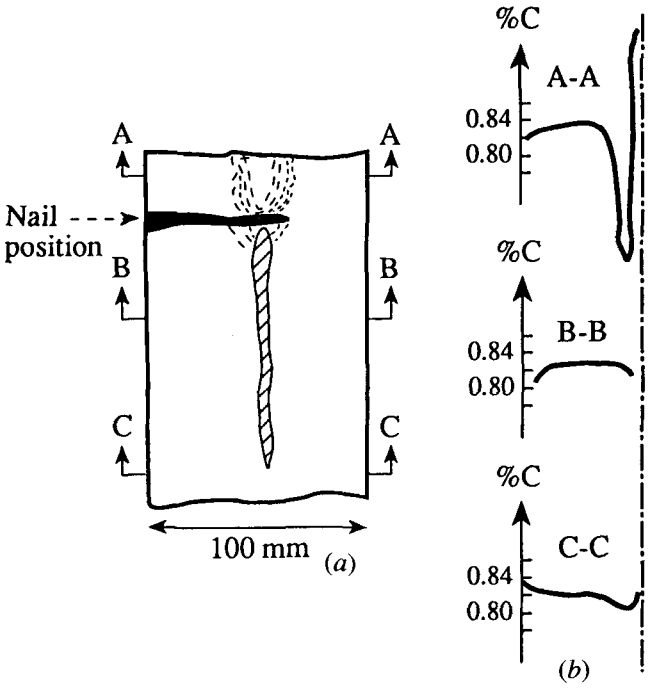

Fig. 5—Segregation analysis for the nailing experiment in Fig. 4.[4]

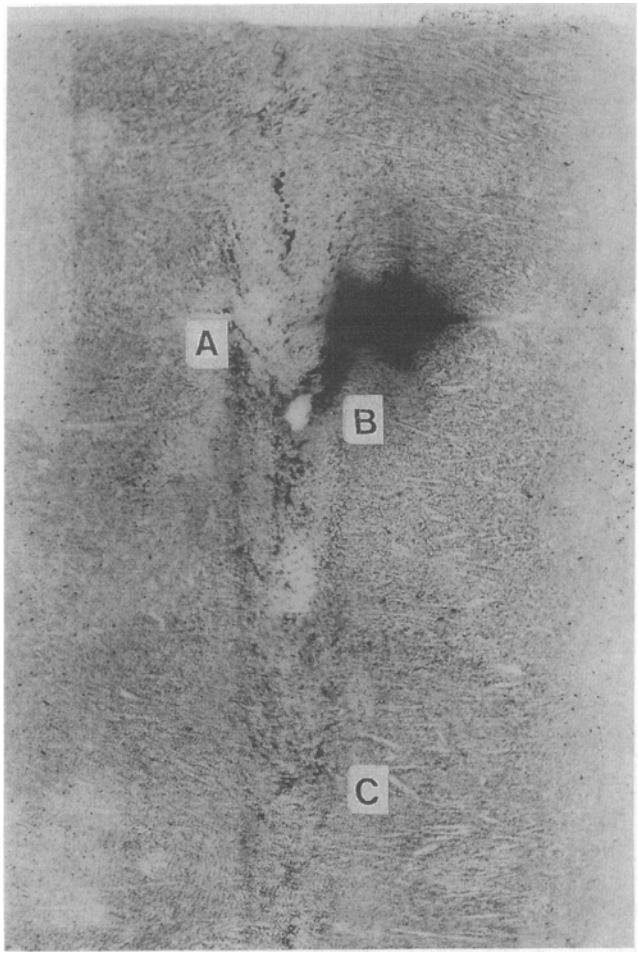

Fig. 6—Downflow of liquid illustrated by a sulfur-doped nail in a sulfur print.[4] A, single V-segregate; B, downward flow; C, packed V-segregates. Magnification 1 times.

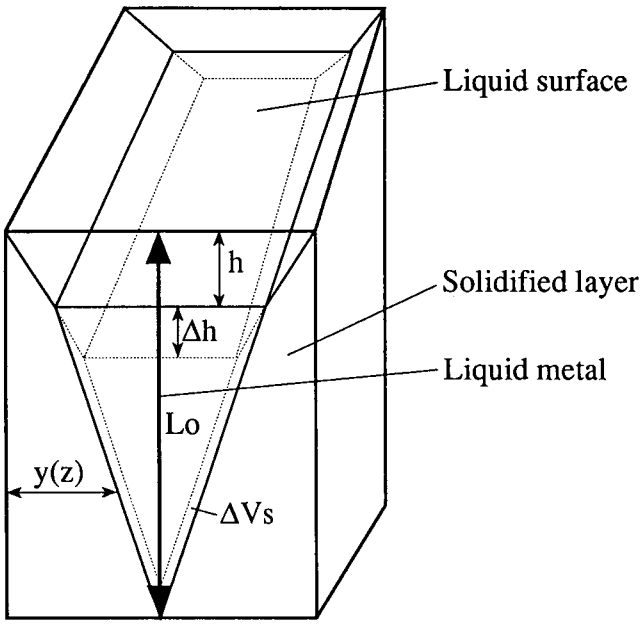

Fig. 7—Volume balance. The liquid surface and the position of the solidification front are shown at two different times, t and $t + \Delta t$.

(m^3), β is solidification shrinkage (negative), dV_c is the difference in the thermal shrinkage volume (m^3), and dt is the time interval in seconds. The left-hand side of Eq. [1] describes the change in depth of the pipe. The first term on the right-hand side describes the contribution due to solidification shrinkage, and the second term the contribution due to thermal contraction.

The first term on the right-hand side will be determined as follows:

$$\left[\frac{dV_s}{dt}\right]_t = \int_{z=h}^{z=L_0} l_l \cdot \frac{dy}{dt}\, dz \qquad [2]$$

where y, h, and L_0 are defined in Figure 7; l_l is the length of the periphery of the solidification front; and y, h, and l_l are functions of z and t. These values are given by a relation describing the solidification process and are found by solving Fourier's heat equation in two dimensions:

$$\frac{\partial T}{\partial t} = \alpha\left[\left(\frac{\partial^2 T}{\partial x^2}\right) + \left(\frac{\partial^2 T}{\partial y^2}\right)\right] \qquad [3]$$

where α is heat diffusivity (m^2/s), T is the temperature in the solidified shell (K), t is time in seconds, and x and y are spatial variables (m).

The rate of heat extraction at the strand surface is given by

$$\frac{dq}{dt} = h(T_s - T_0) = -\omega\left[\frac{dT}{dt}\right]_{y=0} = -\omega\left[\frac{dT}{dx}\right]_{x=0} \qquad [4]$$

where dq/dt is the heat flow per unit area (W/m^2), h is the heat-transfer coefficient (W/m^2 K), T_s is the surface temperature (K), T_0 is the temperature of the surroundings (K), ω is the thermal conductivity (W/mK), and dT/dy and dT/dx are thermal gradients (K/m).

As shown in Figure 1 and Table II, the machines are of a bent type, consisting of the mold and four or five secondary cooling zones. In the calculations, the water flow must be related to a heat-transfer coefficient. In this case, the heat-transfer coefficients in the cooling zones were estimated by using the formula given by Nozaki *et al.*:[7]

$$h = [1.57 \cdot w^{0.55}(1 - 0.0075\theta)]\frac{1}{C_m} \qquad [5]$$

where h is the heat-transfer coefficient (kW/m^2 K), w is the water flux (L/m^2s), θ is the water temperature (°C), and C_m is a machine constant (dimensionless).

The heat-transfer coefficients in the cooling zones at different casting speeds are presented in Tables V and VI. For experiment 1, the heat-transfer coefficient varies linearly with casting speed; for experiment 2, the heat-transfer coefficient is independent of casting speed.

By combining Eqs. [3] and [4] and solving them by an explicit finite-difference method and by using Eq. [2], the first term on the right-hand side of Eq. [1] can be determined. The calculation is divided into time steps (Δt), the strand is divided into height steps (Δz), and for each time the following parameters are calculated:

(1) Position of the solidification front for each z;
(2) Amount of solidified volume for each z;
(3) Area of the liquid for each z;
(4) Total solidified volume; and
(5) New position of the liquid surface.

The position of the solidification front is estimated by defining the corresponding temperature. From the calculated temperature profile obtained by solving Fourier's equation, the position of the front is easily interpolated.

The solidified volume for each z is calculated by taking the difference between the new liquid areas and the old areas, calculated in the previous time step, multiplied by the step length in terms of height. The total solidified volume is the sum of these steps for the entire strand.

We have divided the effect of cooling shrinkage into two parts. One is related to the thermal contraction or expansion due to the temperature changes in the solidified shell before the solidification fronts meet at the center of the strand. The other is related to the contraction or expansion that occurs after the solidification fronts have met at the strand center.

A portion of those contractions occurs by movement of the outer surface inward and a portion by movement of the solidification front outward. Before the solidification fronts meet, the temperature at the front is approximately constant at the liquidus temperature and the temperature at the surface varies. We will therefore assume that the contraction of the solidified layer is localized to the outer surface of the strand before the fronts have met in the central portion. Thus, the contribution of the contraction of the shell to pipe formation before the fronts meet is neglected.

Another situation will occur when the solidification fronts meet at the center of the strand. As is well known, most alloys solidify over a certain temperature interval. The release of latent heat will be spread over this interval and will thus gradually decrease over the interval. The decrease in evolved latent heat will result in a rapid decrease in temperature in the central portion of the strand, while the temperature at the surface of the strand will remain constant or change very slightly (Figure 8). This

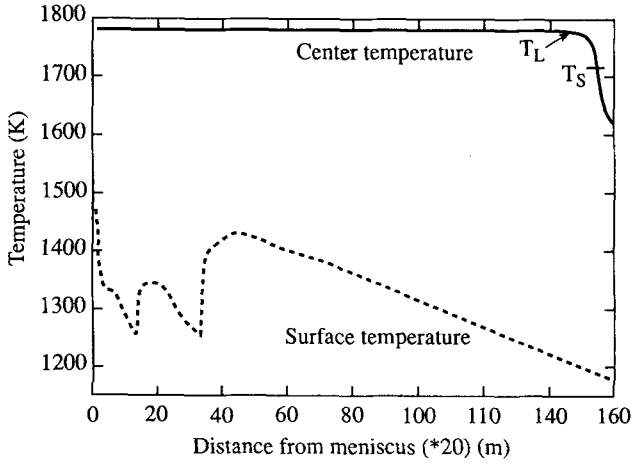

Fig. 8—Temperature at the surface and the center of a continuously cast billet. Note the difference in cooling rate at the end of solidification.

situation is opposite to that which exists during the earlier solidification previously described. The rapid drop in temperature at the center will cause a contraction of the central region. However, the temperature change at the surface will also result in a contraction or expansion of the strand. It is difficult to treat this complex problem either analytically or numerically due to the movement of the boundaries in the central portion as well as the outer surface. Thus, the following simplification was made.

A plate of a strand that follows the strand downward in the casting machine will be studied by dividing the change of the volume of the plate into the following three quantities:

ΔV_{tot} = the total change of the volume due to the thermal expansion or contraction;
$\Delta V_{surface}$ = the total change of the volume due to the thermal expansion or contraction caused by the temperature change at the surface; and
ΔV_{center} = the volume change in the central region.

Since no material is exchanged, the result is

$$\Delta V_{center} = \Delta V_{tot} - \Delta V_{surface}$$

The temperature change with time in the length direction is much smaller than the temperature change with time over the cross section, so we will disregard the contraction change in the length direction and consider only the volume change in the cross section. In this case, we can simplify the calculations to consider only the cross-sectional area, rather than the volume, and thus obtain

$$\Delta A_{center} = \Delta A_{tot} - \Delta A_{surface} \quad [6]$$

The different areas are shown in Figure 9.

The interpretation of Eq. 6 can be described as follows. If ΔA_{center} is positive, then the central portion of the strand is shrinking more than the outer boundary (*i.e.*, the surface) permits. This means that a pore will form in the central region. If, on the other hand, ΔA_{center} is negative, the central portion is shrinking less than the outer boundary. The central region will then be under pressure, and no pore will form.

The area change for the entire area due to the thermal expansion or contraction caused by the temperature change in the entire cross section can be calculated using the following relation:

$$\Delta A_{tot} = 4 \int_{x=0}^{x=x_0/2} \int_{t=t_L}^{t=t_s} 2 \cdot \lambda \cdot \frac{dT(x)}{dt} \left[\frac{x_0}{2} - x \right] dt\, dx \quad [7]$$

where x_0 is the width of the billet (m), t_L is the time when the solidification fronts meet in the center (s), t_s is the time when the center solidifies (s), λ is the thermal expansion coefficient (m^{-1}), and $dT(x)/dt$ is the cooling rate at position x (K/s).

It is more difficult to estimate the area change caused by the temperature change at the outer surface. However, the temperature change at the surface will cause

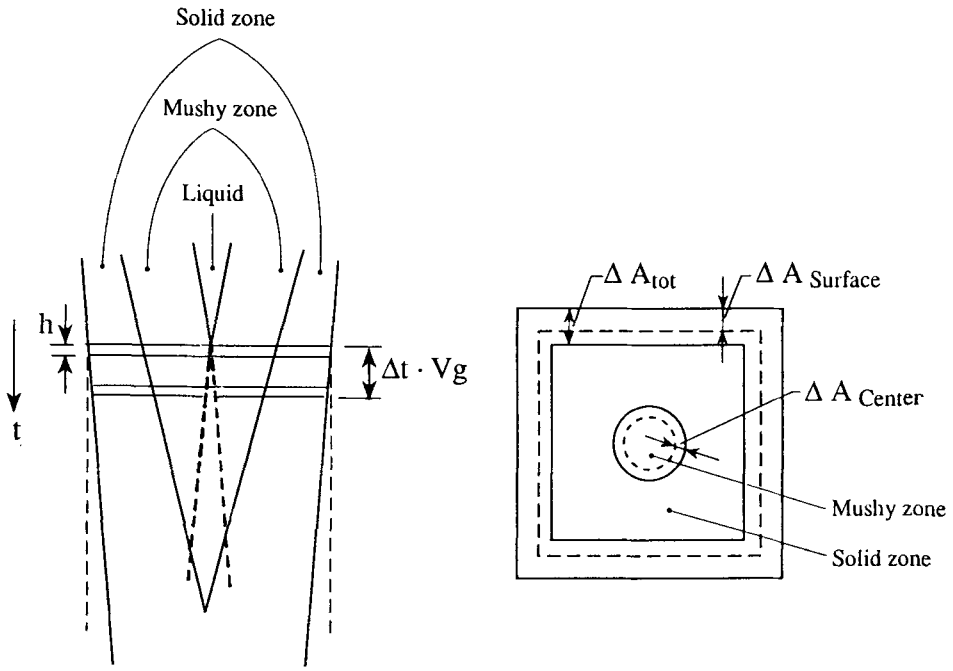

Fig. 9—Schematic illustration of a volume balance for a pore formed by thermal contraction.

the temperature in the interior to change as well. A simple way to consider this would be to say that the temperature change in the interior is a fraction of the distance from the surface. Or, analytically expressed

$$\Delta A_{surface} = 4 \cdot \int_{x=0}^{x=x_0/2} \int_{t=t_L}^{t=t_s} 2 \cdot \lambda \cdot \frac{[(x_0/2) - x]^2}{x_0/2} \cdot \frac{dT_s}{dt} dt \cdot dx \qquad [8]$$

Combining Eqs. [6] through [8] yields the following expression describing the pore size in the central portion of the strand:

$$\Delta A_{center} = 4 \int_{x=0}^{x=x_0/2} \int_{t=t_L}^{t=t_s} \left[2\lambda \frac{dT(x)}{dt} \left[\frac{x_0}{2} - x \right] - 2\lambda \frac{[(x_0/2) - x]^2}{x_0/2} \cdot \frac{dT_s}{dt} \right] dt\, dx \qquad [9]$$

This expression clearly shows that the formation of a pore in the central portion of the strand is very sensitive to temperature change at the surface. If, for example, the cooling rate at the surface dT_s/dt is equal to $dT_{x=0}/dt$, no pore will be formed, because the second term on the right-hand side is larger than the first one. An analytic solution to this differential equation is found by assuming that the temperature varies linearly from the center to the surface. This simplification was used by Engström *et al.*[4]

Equation 9 shows that the cooling rate of the surface significantly influences pore volume. The cooling rate is determined by the casting speed and the cooling conditions. The cooling rates of the strand are calculated, as mentioned earlier, by solving Fourier's equation.

The area change is calculated using Eq. [9] from the moment when the solidification fronts meet (here defined as when the temperature of the center drops 1 K below the liquidus temperature) until the end of solidification (*i.e.*, when the center temperature drops below the solidus temperature). The resulting volume change is estimated as the area of the pore, ΔA_{center}, times the length of the two-phase region in the central portion.

As was shown in Figure 1, the machine used for the experiments is of a bent type. This can result in a backflow of the melt, if it remains liquid in the central portion when the strand is turned horizontally.

The angle between the normal of the liquid surface ($\vec{n}_l$) and the normal of the strand surface ($\vec{n}_s$) decreases from 90 deg when the strand is vertical to 0 deg when the strand is horizontal. This will, of course, influence pipe formation, since the liquid flows backward toward the end of the strand if it has not solidified before it reaches the horizontal position. The formation of the pipe will thus be asymmetric, as was shown in Figure 2. This asymmetry can be further enhanced by the sedimentation of equiaxed crystals.

The effect of the back-flowing liquid on the shape of the pipe can be estimated by a simple assumption. The compensated distance from the meniscus to the liquid surface differs by a distance L from the noncompensated distance (Figure 10). L is calculated as

$$L = \frac{y_s}{2 \tan \gamma} \qquad [10]$$

where γ is the angle between the liquid surface and the solidification front, and y_s is the width of the remaining liquid surface. The compensated distance is then used in describing the lowering of the surface Δh in Eq. [1]. The effect of the sedimenting crystals is more difficult to estimate and will not be considered here.

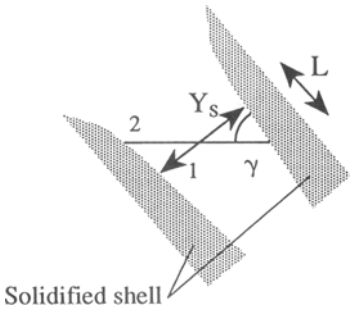

1= Liquid surface without consideration to the bending of the caster.

2= Liquid surface with consideration to the bending of the caster.

L= Compensated distance.

$L = Y_s/(2 \tan(\gamma))$

Fig. 10—Definition of compensated distance, L, where $L = y_s/(2 \tan \gamma)$. 1, liquid surface without consideration of the bending of the caster; 2, liquid surface with consideration of the bending of the caster.

IV. COMPARISON OF THEORETICAL AND EXPERIMENTAL RESULTS

The measured pipe depths in experiments 1 and 2 were compared with the calculated values. The calculations were made for the conditions described in Tables I through VI. At first the calculations were made for a straight casting machine without consideration of the backflow of liquid that occurs when the strand is straightened in a bent caster.

Results of those calculations are shown in Figures 11 and 12, together with experimental results. In Figure 11, the calculation agrees fairly well with the experiment. In this experiment (experiment 1), the casting speed was low enough to avoid backflow of the remaining liquid due to straightening of the strand.

In experiment 2, the casting speed was higher (Figure 12), and the tilting of the strand caused liquid to flow backward. A new calculation was made, taking into consideration the effect of this backflow. The result is shown in Figure 13. As can be seen, the simulation agrees much better with the experiment. The remaining discrepancy may be due to difficulties in estimating the backflow and the formation of equiaxed crystals.

It can be concluded that the casting speed should be decreased toward the end of the casting process; otherwise, the pipe depth will increase because of the backflow of liquid. Another means of decreasing the pipe depth is to reduce the centerline pore by changing the cooling conditions so that the shrinkage of the surface is equal to the volume change of the cross section, as will be discussed later.

V. CENTERLINE MACROSEGREGATIONS

It is well known that the distribution of alloying elements in the central portion of a strand usually follows the pattern shown in Figure 3. This segregation pattern develops as liquid is transported downward to refill the pore formed by thermal contraction during the last part of the solidification process. This liquid transport is illustrated in Figure 6, which also shows the two types of flow patterns: one where the flow is mainly downward and slightly inward, and one where the flow is downward and inward at an angle of roughly 45 deg. The first

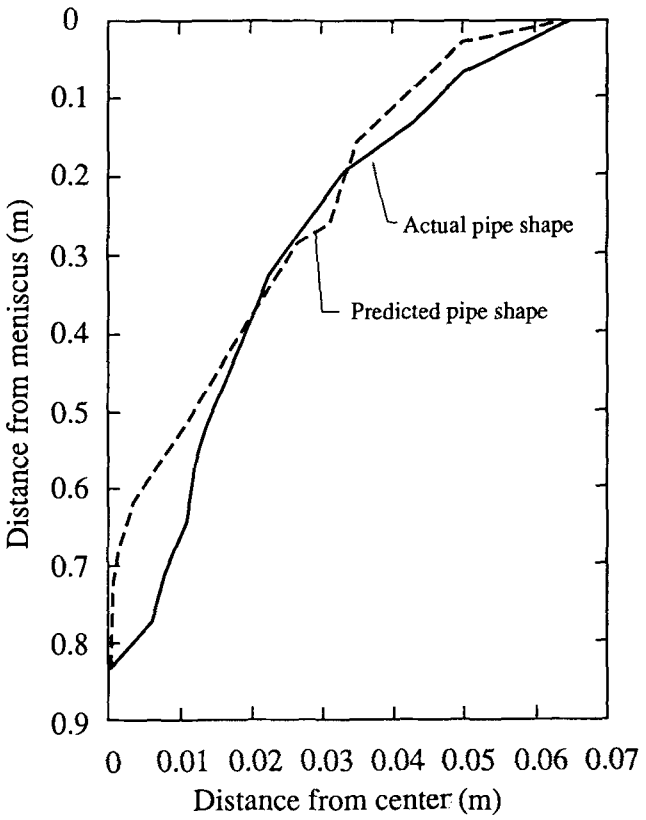

Fig. 11—Actual *vs.* predicted pipe shape in experiment 1.

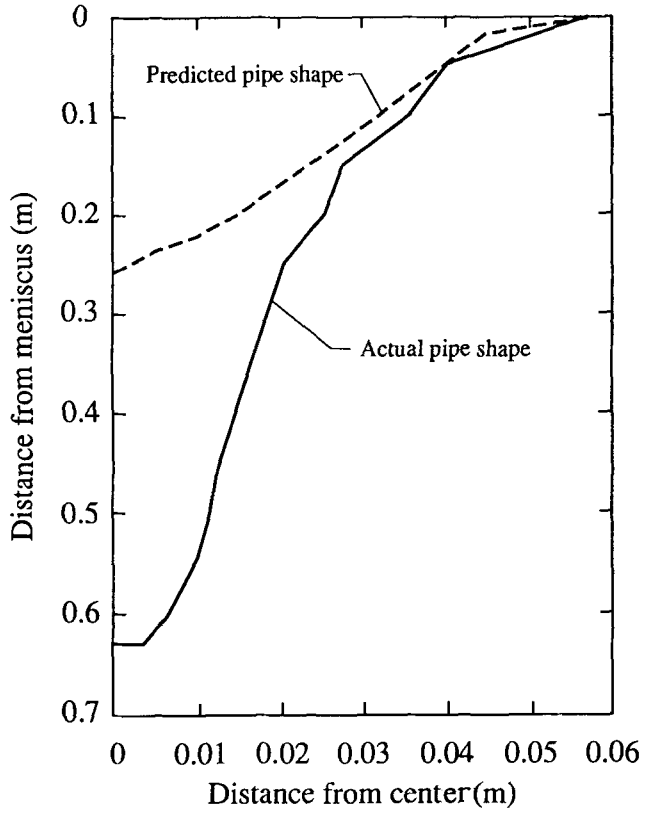

Fig. 12—Actual *vs.* predicted pipe shape in experiment 2.

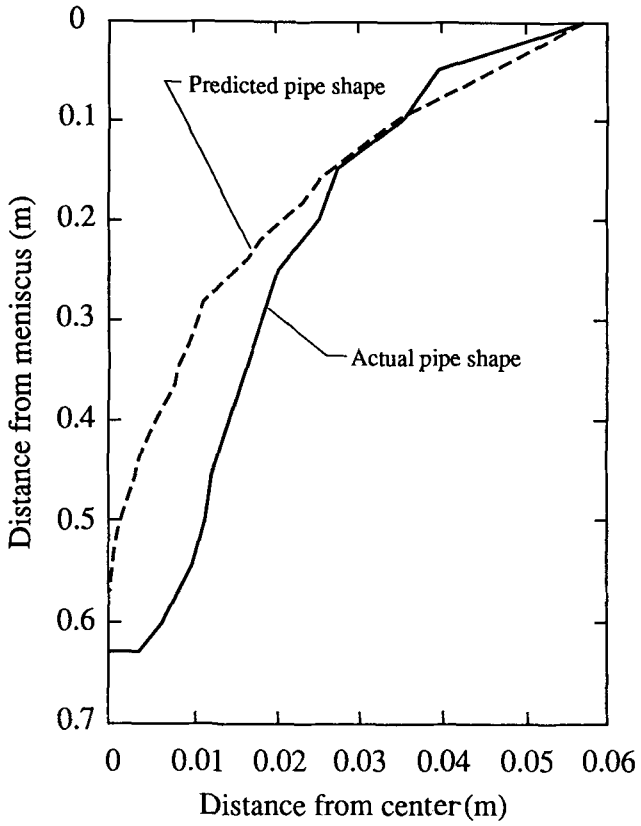

Fig. 13—Actual *vs.* predicted pipe shape in experiment 2, taking into account the effect of backflowing liquid.

flow is caused by the need to fill the pore volume, and the second by the thermal stress in the two-phase region.

The second flow is associated with the formation of V-segregates, as demonstrated by the nailing experiment shown in Figure 6. Two main types of V-segregates occur—namely, single V-segregates and packed V-segregates,[4] both of which are visible in Figure 6. The single V-segregate structure is developed when a material bridge consisting of equiaxed crystals is formed between the two solidification fronts. This material bridge obstructs the downward liquid flow. Upon passing the material bridge, some of the liquid will solidify and be added to the bridge; the alloy concentration in the bridge will thus be lower than the average concentration. Liquid that continues to flow and fill up the pore will consequently be more concentrated.

In some cases, the material bridge grows so large that it totally blocks the liquid transport and a pore starts to form below the bridge. The process is similar to that illustrated by the nailing experiment shown in Figure 4.

When liquid flows downward, its composition changes by either a melting or a solidification process. When the flow is from the upper portion of the strand downward, the composition changes through the freezing of material on the crystals already formed because of the temperature change. The liquid filling the central portion is thus enriched in solute.

A denser pattern of V-segregates is visible in the lower part of Figure 6 (near C). This is more typical when the centerline structure consists of equiaxed crystals. These packed V-segregates are channel-like segregates starting at some distance from the center and are formed when liquid is transported from a colder to a warmer region—a type of transport perhaps caused by thermal stresses. When the temperature begins to drop in the central portion of the strand, the two-phase region becomes compressed, forcing the liquid in this region out into the central portion. It is assumed that compression vectors driving the liquid form an angle of about 45 deg with the downward centerline. The liquid forced downward forms channels in order to find the easiest way out of the two-phase region.

Liquid that flows downward and fills the pore formed in the central portion will be in equilibrium with the solid and will thus change in composition by freezing or melting, depending on whether it flows from a warmer to a colder region or from a colder to a warmer region inside the mushy zone. This knowledge allows the average concentration of the segregated volume in the central portion to be calculated. Calculation begins with the shrinkage pore area, ΔA_{center} (Eq. [9]); we will now try to estimate the average concentration in this volume.

Consider an elementary domain of the mushy zone, the volume of which is V, equal to A times the height h, which adheres to the dendritic tissue of the mushy zone and deforms with it. A reasonable value for A can be the area of the final centerline macrosegregation seen in a sulfur print or an etched sample. The average composition of this domain can be written as follows:

$$\bar{c} = \frac{[\rho^s \cdot A^s \cdot p + A^L \cdot \rho^L]\, C_T^L}{\rho^s \cdot A^s + \rho^L \cdot A^L} \qquad [11]$$

where ρ^s is the density of solid (kg/m^3), A^s is the area of solid (m^2), p is the partition coefficient (negative), A^L is the area of liquid (m^2), ρ^L is the density of liquid (kg/m^3), and C_T^L is the composition of the liquid in equilibrium with the solid at temperature T (w/o).

A change in the volume of the domain, dA, at a fixed temperature will result in a change in its average composition, because liquid will flow in or out of the element to compensate for the volume change. The alloy concentration of the flowing liquid is equal to the alloy concentration of the liquid in the element. This is described the usual way when treating segregation due to shrinkage:[8,9]

$$\bar{c} + d\bar{c} = \frac{[A^s\rho^s p + (A^L + dA)\rho^L]C_T^L}{A^s\rho^s + (A^L + dA)\rho^L} \qquad [12]$$

Combining Eqs. [11] and [12] leads to

$$\frac{d\bar{c}}{C_T^L} = \frac{[\rho^L \cdot A^s \cdot \rho^s][1 - p]dA}{[\rho^s A^s + \rho^L A^L][\rho^L(A^L + dA) + \rho^s A^s]} \qquad [13]$$

By combining Eq. [13] with an expression describing dA and A, the macrosegregation in the central portion of the strand can be calculated. Here, dA is equal to ΔA_{center}, obtained from Eq. [9]. In the following calculations, A is arbitrarily chosen to be 2.5×10^{-5} m^2—corresponding to a pore with a radius of 2.8 mm, which is a reasonable value for the width of a centerline macrosegregation in a billet. A^L and A^S are given by $A^L = A \times g_L$ and $A^S = A - A^L$, and g_L is given by the following relation:[10]

Table VII. Heat-Transfer Coefficients for Hard and Soft Cooling

Cooling Zone	Length of Zone (m)	Heat-Transfer Coefficient (W/m^2 K)	
		Hard	Soft
Mold	0.7	1000	1000
I	1.0	900	700
II	4.3	600	300
III	varying	200	100
Extra cooling zone	varying	600	600

$$1 - g_L = E\left[T_L - T + \frac{2}{\pi(T_s - T_L)}\left(1 - \cos\left\{\frac{\pi(T - T_l)}{2(T_s - T_l)}\right\}\right)\right] \quad [14]$$

where g_L is the fraction of liquid, T_s is the solidus temperature, T_l is the liquidus temperature, T is temperature, and E is equal to $1/[(T_l - T_s)(1 - 2/\pi)]$.

Equation [13] shows that the segregation is significantly influenced by the thermal contraction of the central zone. Two methods for eliminating this contraction have been discussed earlier in the literature: (1) mechanical reduction,[11] which can be broken into several subdivisions ranging from continuous forging, where the reduction ratio can be 30 pct, down to soft reduction, with a reduction ratio of a few percent; and (2) intensive cooling at the end of the liquid pool, or so-called thermal soft reduction. The effect of thermal soft reduction on pipe formation and on centerline macrosegregation has been illustrated by a series of calculations. These calculations assumed that an extra cooling zone was installed at the end of the liquid pool to decrease the difference in cooling rate between the center and the surface of the strand. The material data used are given in Table III.

The calculations were made in order to demonstrate that this type of cooling can minimize the depth of the pipe and the central macrosegregation. The reference frame of the calculations was two different cooling conditions, one hard and one soft, and a constant casting speed for each. The heat-transfer coefficients for the two cooling patterns are shown in Table VII. An extra cooling zone with hard cooling was inserted at the end of the normal secondary cooling zone III (also shown in Table VII). The liquid pool lengths were equal for the different simulations (7.8 m). This was achieved by varying the casting speed between 1.52 and 1.79 m/min, respectively, for soft and hard cooling. The simulations accounted for the effect of thermal shrinkage. The start of the extra cooling zone was varied from the point where the solidification fronts meet to the point where the strand is totally solidified. The extra zone was extended to beyond the end of the liquid pool.

Figure 14 shows that soft cooling results in a shorter pipe than hard cooling. This is because the cooling rate of the surface is higher than that throughout the two-phase region of the central zone, especially at the very end of solidification. Figure 14 also shows that an extra cooling zone always decreases the depth of the pipe if it is extended from the end of zone III to beyond the end of the liquid pool. If the extra cooling zone starts at

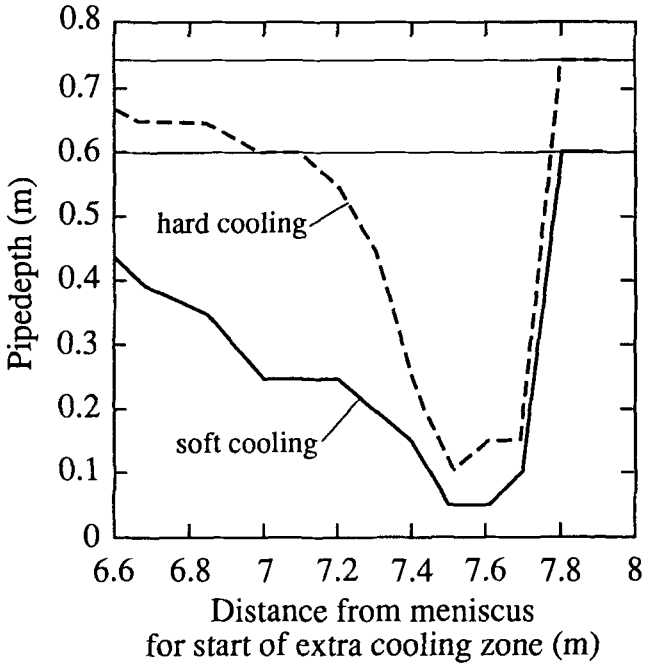

Fig. 14—Variation in pipe depth resulting from the simulated comparison between hard and soft cooling. The two horizontal lines show the pipe depth for hard cooling (0.75 m) and soft cooling (0.6 m) if no extra cooling has been used in the extra cooling zone. Also shown is the optimum location for the extra cooling zone.

7.6 m from the meniscus, the pipe is nearly eliminated. In this case, the depth of the pipe is smaller than that caused by solidification shrinkage. Thermal contraction can thus compensate for solidification shrinkage.

Calculations were also made of the macrosegregation in the central zone (Figure 15). The extra cooling zone has a beneficial effect, decreasing the centerline macrosegregation ratio (C/C_0) for both cooling patterns. The effect is larger for soft cooling. Without extra cooling, soft cooling results in a lower segregation ratio than hard cooling, although the difference is small. It is interesting to note that the contraction of the outer surface can be so large that a negative segregation occurs in the central part, which is the case when the segregation ratio is below 1. Figure 15 also shows that if the extra cooling starts too early, the effect of the extra cooling zone is negative and the segregation ratio increases. This result is consistent with results reported by Jacobson *et al.*,[11] who used a magnetic method to measure the pool depth and found that it was possible to eliminate the centerline segregation by mechanical soft reduction. However,

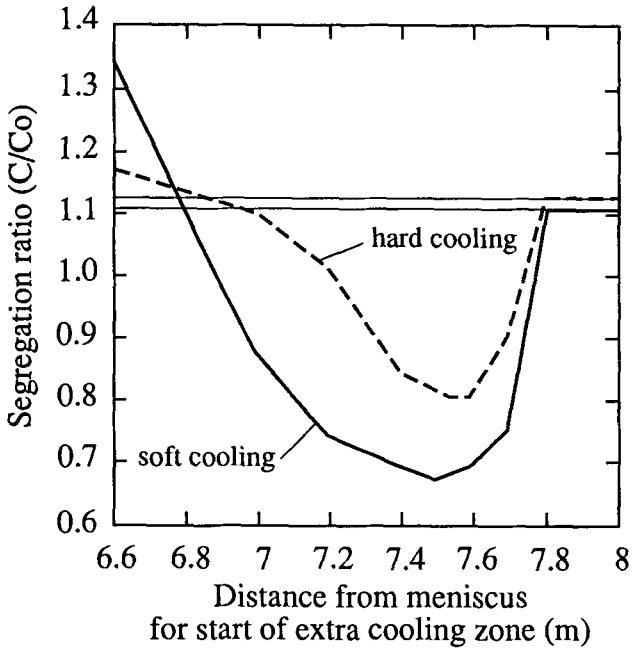

Fig. 15—Centerline macrosegregation ratios resulting from the simulated comparison between hard and soft cooling. The two horizontal lines show the segregation ratios for hard cooling (1.12) and soft cooling (1.11) that resulted when no extra cooling was used during solidification of the last portion of the strand.

they also discovered that the centerline macrosegregation was very sensitive to where and how the reduction took place. It was shown that it is very important to reduce the strand during the last part of the solidification process and to keep the reduction in effect until the strand is totally solidified.

VI. CONCLUDING REMARKS

Pipe formation in continuously cast billets is influenced by the cooling and casting conditions. Thermal contraction plays a major role. In a cooling system where the surface temperature decreases at the same rate as the temperature in the central portion of the strand, thermal contraction can be manipulated to minimize pipe formation.

Shrinkage in the central zones of the strand causes centerline macrosegregation. This can be eliminated by modifying the casting conditions in the same manner used to minimize pipe formation.

REFERENCES

1. H. Mori, N. Tanaka, N. Sato, and M. Hirai: *Trans. Iron Steel Inst. Jpn.*, 1972, vol. 12, pp. 102-11.
2. H. Bauman and W. Löpman: *Wire World Int.*, 1974, vol. 16, pp. 149-55.
3. J.K. Brimacombe and K. Sorimadri: *Metall. Trans. B*, 1977, vol. 8B, pp. 489-505.
4. G. Engström, H. Fredriksson, and B. Rogberg: *Scand. J. Metall.*, 1983, vol. 12, pp. 3-12.
5. C.-M. Raihle, M. Almquist, and H. Fredriksson: Associazone Italiana di Metallurgia, Milano, Italy. 1st European Conf. Continuous Casting, Florence, Italy, 1991.
6. B. Brolund, H. Fredriksson, A. Sunnhagen, and R. West: *Scand. J. Metall.*, 1986, vol. 15, pp. 77-82.
7. T. Nozaki, J. Matsuno, K. Murata, H. Ooi, and M. Kodama: *Trans. Iron Steel Inst. Jpn.*, 1978, vol. 18.
8. E. Scheil: *Metallforschung*, 1947, vol. 2, p. 69.
9. M.C. Flemings and G.E. Nereo: *Trans. TMS/AIME*, 1967, vol. 239, p. 1449.
10. B. Rogberg: Doctoral Thesis, Royal Institute of Technology, Stockholm, Sweden, 1982.
11. N. Jacobson, C.-M. Raihle, and N. Leskinen: *Scand. J. Metall.*, 1992, vol. 21, pp. 172-80.